

METAL-BASED THREE-DEGREE-OF-FREEDOM ACTUATOR WITH SHAPE MEMORY

¹FAUSTO RAMIRO CABRERA AGUAYO, ²DIEGO RAMIRO ÑACATO ESTRELLA, ³FABRICIO JAVIER SANTACRUZ SULCA, ⁴ERICK PATRICIO MENESES CASQUETE, ⁵WILSON IGNACIO CAMPOVERDE PABON, ⁶OSCAR CURET

¹Florida Atlantic University (FAU)

Guest Researcher, Department of Ocean and Mechanical Engineering
frca.cabrera@epoch.edu.ec

<https://orcid.org/0000-0002-0816-155X>

²Escuela Superior Politécnica de Chimborazo (ESPOCH)

Facultad de informática y electrónica

Carrera Electrónica y Automatización

diego.nacato@epoch.edu.ec

<https://orcid.org/0000-0002-7233-9076>

³Escuela Superior Politécnica de Chimborazo (ESPOCH)

Facultad de informática y electrónica

Carrera Telecomunicaciones

fabricio.santacruz@epoch.edu.ec

<https://orcid.org/0000-0001-7123-2552>

⁴Investigador Independiente

meneeses.erick@hotmail.com

<https://orcid.org/0009-0005-6065-0616>

⁵Investigador Independiente

wilo_sss@hotmail.com

<https://orcid.org/0009-0001-5928-6512>

⁶Florida Atlantic University (FAU)

Associate Professor, Department of Ocean and Mechanical Engineering
ocuret@fau.edu

<https://orcid.org/0000-0002-3202-6841>

Abstract: Implemented a three-degree-of-freedom actuator using shape memory metals (SMA) for two-dimensional motion. In its design, CAD software was used to analyze the movements made by a ball joint, obtaining a conical body with a circular base. For its movement, a single-way SMA spring arrangement was implemented as opposed to a two-way arrangement for displacement in each of the XY axes, and its rotation by means of a bearing coupled to the axis of the body that allows the rotation in one direction of the actuator. An on-off control was implemented based on a kinematic study that can be manipulated through an interface that, according to the temperature and position obtained, activates or deactivates the SMA elements. As a result, the angle of work was determined in a two-dimensional plane of $\pm 22.5^\circ$ and 30° counterclockwise for its rotation taking into account that its error grows as it moves away from its center.

Abstract: A three-degree-of-freedom actuator was implemented using shape memory metals (SMA) for two-dimensional movement. In its design, a CAD software was used, analyzing the movements made by a ball joint, obtaining a conical body with a circular base. For its movement, a one-way SMA spring arrangement was implemented as opposed to a two-way one for displacement in each of the XY axes, and its rotation by means of a bearing coupled to the axis of the body that allows rotation in one direction. actuator. An on-off control was implemented based on a kinematic study that can be manipulated through an interface that, according to the temperature and position obtained, activates or deactivates the SMA elements. As a result, the working angle was determined in a two-dimensional plane of $\pm 22.5^\circ$ and 30° counterclockwise for its rotation, taking into account that its error grows as it moves away from its center.

Keywords: actuator, SMA, manipulated, conical



I. INTRODUCTION

AndThe use of conventional actuators limits the possibilities of equipment design due to the characteristics they have such as their structure or weight, so the use of unconventional actuators is presented as an alternative to generate the same type of movement. [1]

Biomedical studies catalog muscles as an ideal model of actuation system, which is why it has been decided to investigate the camp or artificial muscles based on shape memory alloys or SMA for its acronym *Shape Memory Alloy*, specifically made based on Nickel and Titanium called Nitinol,[2] which has received great reception due to its biocompatibility, malleability and ductility, stability against cyclic applications, and its shape memory because these alloys can be deformed and return to their original state after heating.[3] At present, its use is reflected in areas such as medicine, robotics, automation or space engineering.

Commercially there are SMA actuators that although they show an excellent ratio of force - weight, their range of movement is small and have a single degree of freedom.[4] In the research area, several projects have been developed such as the realization of a pectoral fin driven by SMA based on the Koi carp fish, which through a current PWM allows a bending movement of 2 GDL, in the area [5]of flexible robotics a continuous robot has been developed that based on three silicone segments and the use of Nitinol seeks to suppress rigid elements that are part of other actuators[6], or an actuator with ball joint link that allows 2 GDL through a diffuse PID control and the use of three pairs of antagonistic SMA cables obtaining a movement of $\pm 60^\circ$ [7].

Through this research, the development of an actuator that through the temperature control of Nitinol springs allows movement in a rotating two-dimensional plane obtaining 3 GDL was sought, in addition to being able to determine its position and orientation with the help of a developed interface.

Fig. 1 shows a general design of the actuator conformation, based on a ball joint next to a link, the end of which is the point that indicates its position and final orientation.

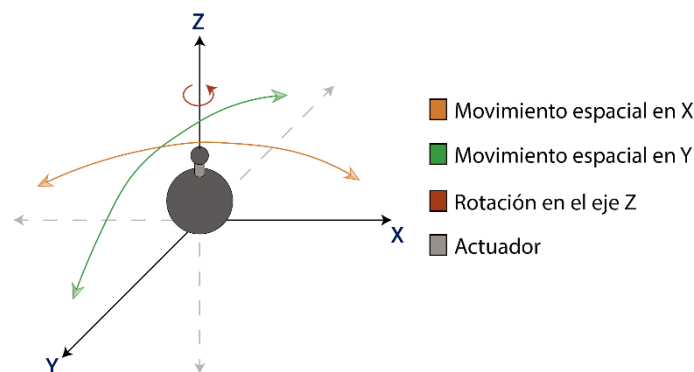


Fig. 1. General design of the proposed movements of the actuator.

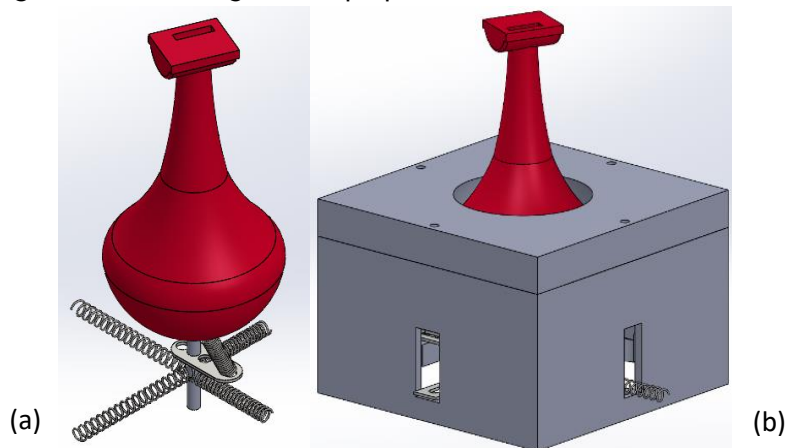


Fig. 2. Structural design of the actuator: (a) Body with the placement of the different springs for its movement, (b) Base of the actuator.



II. NITINOL SPRINGS

The SMA elements have their characteristic behavior due to the austenitic - martensitic transformation that causes the rearrangement of atoms by deformation without their migration, which [8] is why having the shape of a coil spring exists and greater amount of wire, having a greater total stretch.

The company Nexmetal presents two types of springs, when its Nitinol structure is 1 way it can contract or expand according to its engraving, and generate a force of up to 400 g when it reaches ; and when its Nitinol structure is 2-way, when it reaches a temperature of it can expand or contract according to its engraving 60°C 60°C, and when lowering its temperature to 30°C resumes its initial position, being for this case unnecessary the realization of a physical force on it [9].

III. DESIGN OF THE MECHANICAL STRUCTURE

Based on the movements that are sought to be obtained, we opted for the realization of two main bodies, the body that acts as the actuator, and a base on which it performs its movements. Its body has a spherical base that emulates the movements of a kneecap, and the rest of its body a conical shape as a link with ducts that allows to place an end effector, or in this case a position sensor to obtain feedback from its location.

The movement of the body is carried out based on an axis that crosses its center, which allows the location of the different springs as follows: For the movement on the X axis and on the Y axis, two Nitinol springs are available for each axis placed in opposition so that when the first spring contracts when heated its opposite expands by physical action, and when its actuation is opposite, its movement to be made is the opposite.

For the movement on the Z axis, a bearing is used at the base of the body and an aluminum sheet that allows the expansion and contraction of the two-way SMA spring, generating a rotary movement counterclockwise, and when cooling the return to its initial position.

Fig. 2 shows the design of the actuator body in conjunction with the location of the various SMA springs, and the placement on their base.

IV. ACTUATOR KINEMATIC STUDY

The movement of an actuator is based on the joints of a living being, such as the shoulder that has 3GDL where its two main movements are the elevation in a scapular plane, and the rotary movements [10], that is why based on these movements and the design of its mechanical structure we proceed with the kinematic analysis of the same considering its movements in the order X-Y-Z.

A. Direct actuator kinematics

For the first case, a motion analysis is performed with respect to the fixed reference frame where the rotation of each axis is performed with respect to this system resulting in (1), which once solved obtains the homogeneous transformation matrix (2), which contains the Euler rotation matrix with the addition of a translation on Z.

$$T = T(0,0, d_1)Rotz(\theta)Roty(\phi)Rotx(\alpha) \tag{1}$$

$$T = \begin{bmatrix} C_\phi C_\theta & S_\alpha S_\phi C_\theta - C_\alpha S_\theta & S_\alpha S_\theta + C_\alpha S_\phi C_\theta & 0 \\ C_\phi S_\theta & C_\alpha C_\theta + S_\alpha S_\phi S_\theta & C_\alpha S_\phi S_\theta - S_\alpha C_\theta & 0 \\ -S_\phi & S_\alpha C_\phi & C_\alpha C_\phi & d_1 \\ 0 & 0 & 0 & 1 \end{bmatrix} \tag{2}$$

In a second analysis is performed with respect to a mobile reference system, where the rotation of each axis is performed consecutively with respect to this system in the order U-V-W resulting in the composition (3), which developed results in the homogeneous transformation matrix (4).

$$T = Rotu(\gamma)Rotv(\delta)Rotw(\varphi)T(0,0, d_1) \tag{3}$$



$$T = \begin{bmatrix} C_\delta C_\varphi & -C_\delta S_\varphi & S_\delta & S_\delta d_1 \\ S_\gamma S_\delta C_\varphi + C_\gamma S_\varphi & C_\gamma C_\varphi - S_\gamma S_\delta S_\varphi & -S_\gamma C_\delta & -S_\gamma C_\delta d_1 \\ S_\gamma S_\varphi - C_\gamma S_\delta C_\varphi & C_\gamma S_\delta S_\varphi + S_\gamma C_\varphi & C_\gamma C_\delta & C_\gamma C_\delta d_1 \\ 0 & 0 & 0 & 1 \end{bmatrix} \quad (4)$$

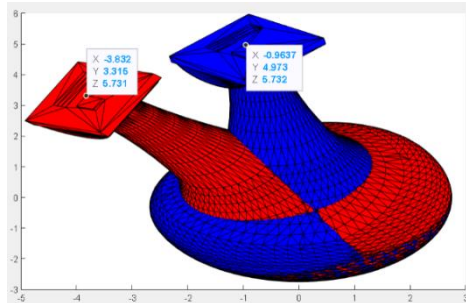


Fig. 3. Study of spatial movement of the actuator based on the mobile reference system (red) and a fixed reference system (blue).

Espacio de trabajo del actuador

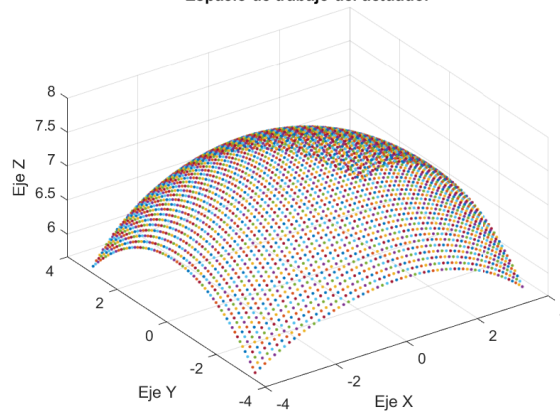


Fig. 4. Theoretical workspace with limitation for the angles of X and Y $\pm 30^\circ$ obtaining a total of 3721 possible positions of the actuator end.

Fig. 3 allows us to show graphically each of the analyses mentioned above, where when placing at the angles $\gamma = -30^\circ$ moving reference system and $\delta = -30^\circ$ a distance, one reaches the XYZ position $d_1 = 7.55 \text{ cm}$ shown by the red body, while placing $(-3.83; 3.31; 5.73) \text{ cm}$ the angles $\alpha = -30^\circ$ $\phi = -30^\circ$ and n base to a fixed reference frame the XYZ position shown by the blue body $(-0.95; 4.97; 5.73) \text{ cm}$ is obtained. As evidenced by the reference system used when placing the same angles, one position or another is reached; For this case the second analysis is better adapted to the expected movements of the actuator due to the placement of its springs.

To proceed with obtaining your theoretical workspace shown in Fig. 4 The extent of its motion was limited to its angles and to γ since its position in space depends exclusively on these two data δ , and for $\pm 30^\circ$ the 30° counterclockwise angle to determine its rotation.

B. Inverse actuator kinematics

Once obtained its direct kinematics can obtain its inverse kinematic model based on (5) where the elements of the homogeneous transformation matrix are identified, and by taking the inverse matrix of each of the components in (3) it is possible to find each of the angles based on the product of matrices where relationships are obtained between the position of each matrix, taking into account those that express the angle sought as a function of constants.

$$T^{-1} = \begin{bmatrix} \mathbf{n} & \mathbf{o} & \mathbf{a} & \mathbf{p} \\ 0 & 0 & 0 & 1 \end{bmatrix}^{-1} = \begin{bmatrix} n_u & n_v & n_w & -\mathbf{n}^T \mathbf{p} \\ o_u & o_v & o_w & -\mathbf{o}^T \mathbf{p} \\ a_u & a_v & a_w & -\mathbf{a}^T \mathbf{p} \\ 0 & 0 & 0 & 1 \end{bmatrix} \quad (5)$$



Once these relationships have been obtained and their mathematical development is carried out to find each of the solutions, the expressions shown in (6), (7) and (8) are obtained.

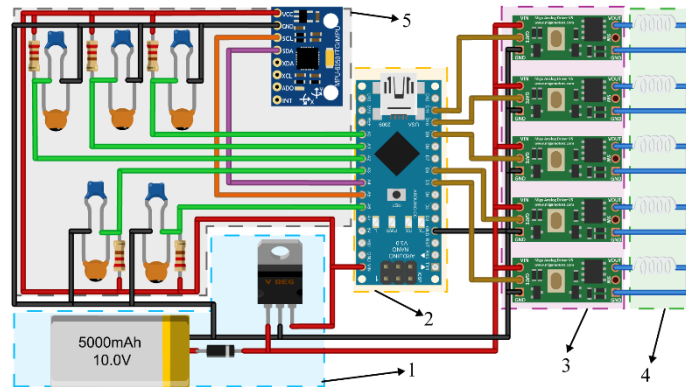


Fig. 5. Actuator control circuit. [1) Power block. 2) Processing block. 3) Control drivers. 4) SMA springs. 5) Sensor block.]

$$\gamma = -\tan^{-1}\left(\frac{p_v}{p_w}\right) \tag{6}$$

$$\delta = -\tan^{-1}\left(\frac{p_u}{p_v S_\gamma - p_w C_\gamma}\right) \tag{7}$$

$$\varphi = \sin^{-1}(n_v C_\gamma + n_w S_\gamma) \tag{8}$$

CONTROL CIRCUIT

The actuator motion control was used various hardware elements shown in Fig. 5, divided into 5 blocks to explain its functioning.

Its process begins with the power required for the prototype, a 10V to 5A supply for the activation of the SMA elements, and a voltage regulator 7805 for the power of the electronic components, then in the processing block there is an Arduino Nano for the execution of commands for the control of the actuator that sends data to the driver block where MADv5 controls various SMA springs using a Gate signal. Data collection is carried out using the sensor block with the help of five NTC Murata thermistors for obtaining temperature from the SMA springs and an MPU6050 gyroscope and accelerometer for obtaining position, orientation, speed and acceleration at the end of the actuator.

CONTROL AND MONITORING ALGORITHM

For its development, certain requirements were taken into consideration, such as the control of start and stop of the actuator, sending PWM signals to the driver block according to the required movements, and the collection of data from the thermistor and the MPU6050 for visualization and monitoring.

Fig. 7 shows the general scheme of the actuator, where a closed loop system is observed between the ball joint and gyroscope, in order to reach the indicated position with the help of SMA springs, its process is explained in detail below.

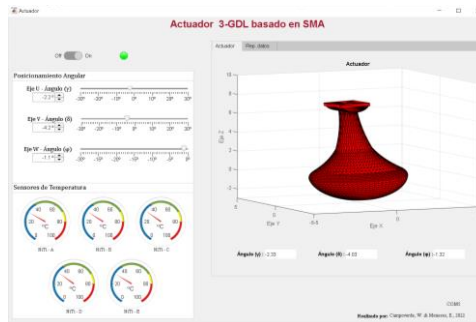


Fig. 6. Controland monitoring interface developed.

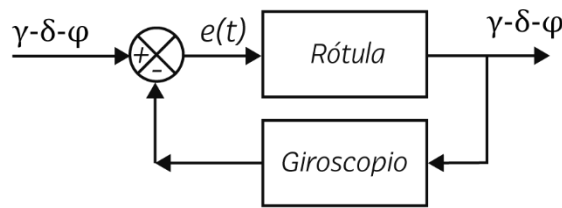


Fig. 7. Closed loop actuator system

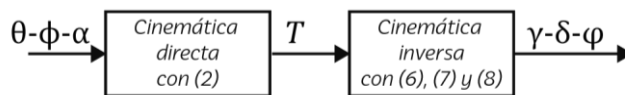


Fig. 8. Angle conversion by applying direct and reverse kinematics.

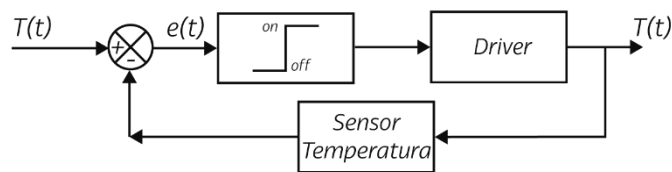


Fig. 9. Control on - off for the actuation of each of the SMA springs by means of control drivers.

In order to be able to send the position data and monitor all these variables, the interface shown in Fig. 6 was developed, where after turning on and placing the degrees of movement for each axis, it allows to observe the movement made by the actuator in real time. While observing the temperature of each SMA spring, all this through a serial communication from Arduino.

Since the gyroscope works with Euler angles it is necessary to convert based on the required angles, Fig. 8 shows this process where the angles obtained or s of the MPU6050 are applied in (2) to obtain its homogeneous transformation matrix, and then based on (6), (7) and (8) obtain the value of the angles as a function of $\gamma - \delta - \phi$.

The angles obtained are compared with its input, if the angle is lower, the SMA spring that is anchored to the positive part of the axis is activated, and if the angle obtained is greater, its opposite is activated; taking into account that the maximum value that the SMA element must reach is to 60°C avoid re-engraving of its structure or other damage. To move each of these springs, an on-off control shown in Fig. 9 where based on the temperature at which it reaches its position, and the temperature read by the thermistor activates and deactivates its controller keeping it in the indicated position.

CALIBRATION OF SENSORS AND VARIABLES

A. Tarjeta GY - 521 with MPU6050

To obtain data from this element is recommended the use of a library that allows greater ease of programming, so tests were carried out with libraries <MPU6050_light.h> and <TinyMPU6050.h>, their data obtained were compared with a conveyor obtaining as a result less measurement error with the use of the 360° second library.

B. Murata temperature sensor

Being a resistive component, a conditioning circuit is required that allows the reading of voltage in its terminals by means of a voltage divider with a potentiometer of 10 kΩ, as shown in Fig. 5, and the data obtained is applied in (9) that relates the temperature in degrees Celsius with respect to the voltage.

$$T = -0.30779 V^5 + 4.1545 V^4 - 23.272 V^3 \tag{9}$$



$$+68.015 V^2 - 126.35 V + 150.42$$

C. Nitinol activation response

Since using a PWM power supply achieves a better heat distribution and better energy consumption, and tomado in account as the main parameter the total activation of the SMA element in a time close to 20s to avoid the temperature overelongation reached, it was carried out tests at different values of *Dutty Cycle*, obtaining an optimal value at 23% with a voltage of 0.64V and current of 0.62 A for a spring.

PROTOTYPE VALIDATION

Once the prototype was implemented, motion tests were carried out on one, two and three axes to check the error that reaches the form of increasing the number of springs for each movement.

A. Movement around the U-axis

To evaluate this movement based on the U axis of the mobile reference system, a total of 25 samples were made where the position error was calculated based on the theoretical data obtained, having a maximum error of 2.57% produced when moving the angle γ 30°. Fig. 10 graphically shows each of the samples obtained in space (blue), and the theoretical points to be reached (red) foreach sample.

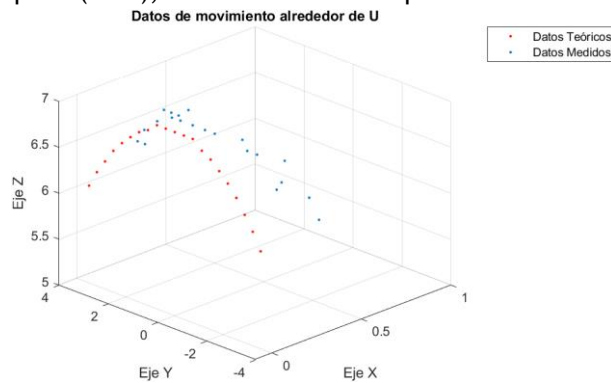


Fig. 10. Activation response of the theoretical angle and obtained γ .

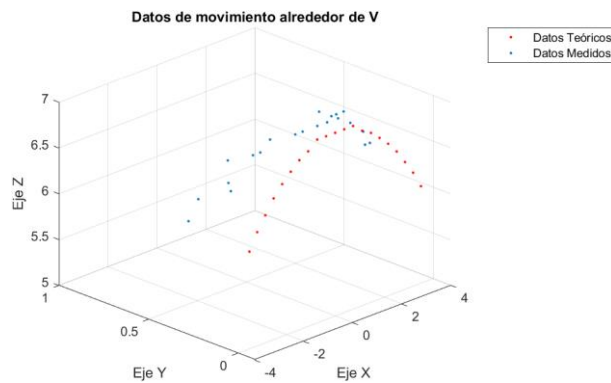


Fig. 11. Activation response of the theoretical angle and obtained δ .

B. Motion around the V-axis

The evaluation of the movement based on the V axis of the mobile reference system was carried out with a total of 25 samples where a maximum position error of 2.55% produced when moving the angle δ to its end was calculated. Fig. 11 graphically shows each of the samples obtained in space (blue), and the theoretical points to be reached (red) for each sample.

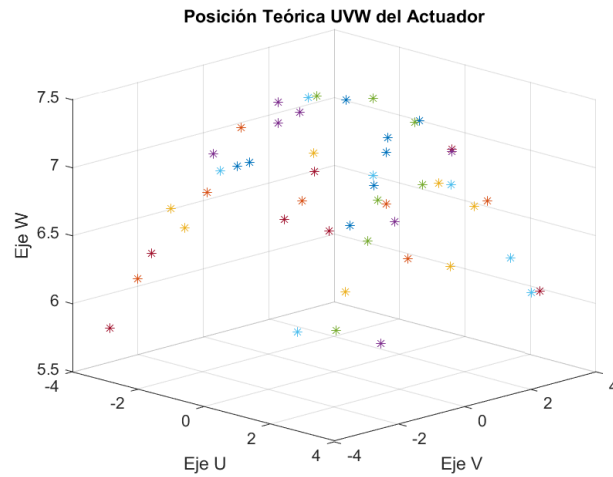


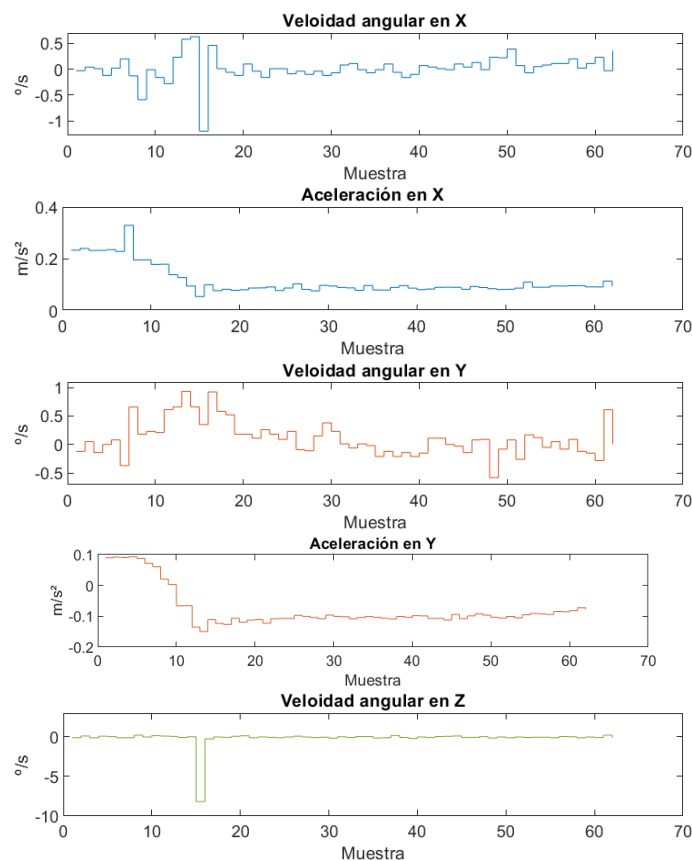
Fig. 12. Activation response of the theoretical angle and obtained γ .

C. Two-axis movement

The position of the actuator is determined by the angles and, so it is important to evaluate whether when entering their respective values, the device performs a movement $\gamma\delta$ according to its theoretical position. Based on this, 50 samples were analyzed, which are shown in Fig. 12, obtaining a maximum error of 2.63%

D. Movimientor three-axis

When performing this movement apart from the translation, the rotation of the body intervenes on its basis in a mobile reference system, so its position and rotation for each sample was analyzed, based on this a maximum error of 3.86% was obtained, which in comparison to the error obtained during the movement in the U-V axes, It is greater, this is because by increasing the rotational degree, it causes a greater involuntary movement of the angles γ and δ .



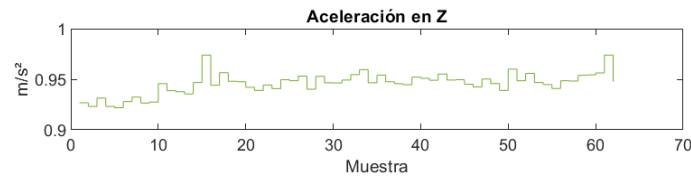


Fig. 13. Angular velocity and acceleration generated in the X - Y - Z axes of the actuatedr.

E. Acceleration and applied speeds

Fig. 13, shows the speed and acceleration obtained during the movement in each of its axes one, where it is observed that neither of the two is constant and have peaks in it, this is due to friction between the base of the device and its body, the material in which it is manufactured since 3D printing is not entirely compact or uniform due to the layered destruction in which it is made.

In addition, it is observed that on average its speed is half a degree per second for the X and Y axes, while for the Z axis it is almost zero. Its acceleration, on the other hand, stabilizes as time progresses, having its maximum at the beginning of the movement, for the X and Y axes; for the Z axis instead it remains mostly stable according to the acceleration of gravity.

CONCLUSIONS

A three-degree of freedom actuator was implemented using springs with shape memory for movement in a rotating two-dimensional plane covering the need for the use of unconventional elements, obtaining activation and control data of the SMA elements used by means of an inertial and temperature measurement sensor, which allows evidence that the position can be determined effectively.

A digital model of the actuator was obtained that has a link that allows rotational movements for displacement in a two-dimensional plane.

The coupling with bearing is an effective alternative for actuator rotation control, and a spring arrangement that allows movement in a two-dimensional plane.

The implementation of a temperature control system allows to control the position of the actuator, all this through a graphical interface.

The IMU card generates reading errors due to decalibration that increases with the passage of time

REFERENCES

- [1] A. Gómez and C. A. Restrepo, "MUSCULAR CABLES", *Revista EIA*, no. 4, pp. 103-111, 2005, Accessed: Nov. 11, 2021. [Online]. Available: http://www.scielo.org.co/scielo.php?script=sci_arttext&pid=S1794-12372005000200010&lng=en&nrm=iso&tlng=es
- [2] A. Cano Sánchez, "Estudio e implementación de actuadores basada en aleaciones SMA", Madrid, Oct. 2010.
- [3] S. de la F. López, "Numerical simulation and experimental correlation of mechanical properties in shape memory alloys.", *TDX (Doctoral Thesis in Xarxa)*, jun. 2005, Accessed: Nov. 04, 2021. [Online]. Available: <http://www.tdx.cat/handle/10803/6863>
- [4] International Organization for Shape Memory and Superelastic Technologies, "Shape Memory Alloy Bonds: Shape Memory and Superelastic Technologies," 2022. <https://www.asminternational.org/web/smst/shape-memory-alloys-links> (accessed May 01, 2022).
- [5] S. Zhang, B. Liu, L. Wang, Q. Yan, K. H. Low, y J. Yang, "Design and implementation of a lightweight bioinspired pectoral fin driven by SMA", *IEEE/ASME Transactions on Mechatronics*, vol. 19, núm. 6, pp. 1773-1785, dic. 2014, doi: 10.1109/TMECH.2013.2294797.
- [6] M. Guzmán Merino, "CONTINUOUS ROBOT ACTUATED WITH SMA", Polytechnic University of Madrid, Madrid, 2020.

- [7]Z. Shi, T. Wang, D. Liu, C. Ma, y X. Yuan, "A fuzzy PID-controlled SMA actuator for a two-DOF joint", *Chinese Journal of Aeronautics*, vol. 27, núm. 2, pp. 453-460, abr. 2014, doi: 10.1016/J.CJA.2014.02.015.
- [8]D. A. Rodríguez Espitia, A. N. Martínez Soto, A. F. Rojas Cortés, and M. Medina Devia, "Materiales Inteligentes", Bogotá, jul. 2019. Accessed: Nov. 24, 2021. [Online]. Available: <https://vsip.info/materiales-inteligentes-5-pdf-free.html>
- [9]Nexmetal Corporation, "Nitinol 2-Way Memory Coil Spring W0.75 x D6.5 x C16; Af 55", 2022. <https://nexmetal.com/collections/nitinol-springs/products/nitinol-2-way-memory-spring-w075-d65> (consultado jun. 07, 2022).
- [10]N. Suárez Sanabria and A. M. Osorio Patiño, "Biomechanics of the shoulder and physiological bases of Codman's exercises", *CES Medicina*, vol. 27, no. 2, pp. 205-217, Apr. 2013, Accessed: Nov. 11, 2021. [Online]. Available: <http://www.scielo.org.co/pdf/cesm/v27n2/v27n2a08.pdf>